Accepted Manuscript

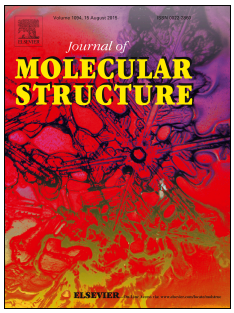

Modeling molecular interactions of propounded pyrazole based drug candidates against bacterial DNA gyrase: Validation by syntheses and biological studies

Shubhangi, Nikhil Kumar, Rajendiran Kanagaraj, Kashmiri Lal, Avijit Kumar Paul

PII: S0022-2860(19)30697-0

DOI: https://doi.org/10.1016/j.molstruc.2019.05.125

Reference: MOLSTR 26632

To appear in: *Journal of Molecular Structure*

Received Date: 26 April 2019

Revised Date: 28 May 2019

Accepted Date: 28 May 2019

Please cite this article as: Shubhangi, N. Kumar, R. Kanagaraj, K. Lal, A.K. Paul, Modeling molecular interactions of propounded pyrazole based drug candidates against bacterial DNA gyrase: Validation by syntheses and biological studies, *Journal of Molecular Structure* (2019), doi: https://doi.org/10.1016/j.molstruc.2019.05.125.

Graphical Abstract

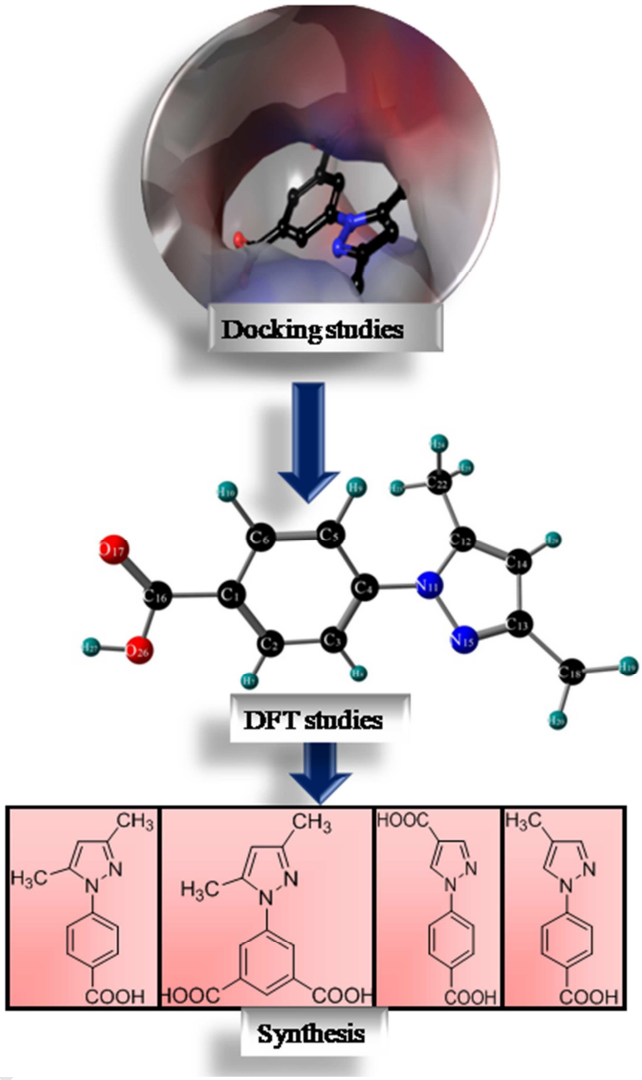

Modeling molecular interactions of propounded pyrazole based drug candidates against bacterial DNA gyrase: Validation by syntheses and biological studies

Shubhangi[1†], Nikhil Kumar[1†], Rajendiran Kanagaraj[1], Kashmiri Lal[2] and Avijit Kumar Paul[1]*

[1]Department of Chemistry, National Institute of Technology Kurukshetra, Kurukshetra-136119, Haryana, India.

[2]Department of Chemistry, Guru Jambheshwar University of Science and Technology, Hisar-125001, Haryana, India.

Keywords: Substituted pyrazoles; Docking studies; DNA gyrase; Antimicrobial activity; DFT study.

†: Both the authors contributed equally

* Email id: apaul@nitkkr.ac.in

Abstract

A class of nitrogen-based heterocycles, pyrazoles and their derivatives, are cardinal agents in the field of pharmacology. Here, we have conducted *in silico* studies on newly designed pyrazole based drug molecules, thereby revealing their activities and interaction behaviors when docked against *S. aureus* DNA gyrase upon comparison with a standard drug ciprofloxacin and previously reported few compounds. The drug likeliness of the compounds was analyzed using QikProp module of *Maestro 11.5* (Schrödinger) through ADME (Absorption, Distribution, Metabolism and Excretion) analysis. Among the predicted compounds, we have synthesized four pyrazole derivatives; namely 5-(3, 5-dimethyl-1H-pyrazol-1-yl) 1,3-benzoic acid, 5-(3, 5-dimethyl-1H-pyrazol-1-yl) 1,3-benzenedicarboxylic acid, 4-(4-methyl-1H-pyrazole-1-yl) benzoic acid and 1-(4-carboxyphenyl)-1H-pyrazole-4-carboxylic acid. All the four compounds are characterized by ^{1}H and ^{13}C NMR, IR, UV, and mass spectrophotometry. We have successfully tested the same compounds for anti-microbial activities involving testing with standard bacterial as well as fungal strains. Anti-bacterial activity testing was performed against two Gram-positive bacteria: *Staphylococcus aureus*, *Bacillus subtilis* and three Gram-negative bacteria: *Escherichia coli*, *Pseudomonas aeruginosa*, *Salmonella enterica*. Anti-fungal activity was carried out against a well-known fungal strain *Candida albicans*. The observed antimicrobial activities are in well agreement with the docking results. The DFT study was also carried out to compare the conformational stability of the optimized structures and docked-pose of the four molecules.

1. Introduction

Biologically active heterocycles, namely oxadiazoles, triazoles, thiadiazoles or pyrazoles, have been widely used for therapeutics [1–3]. The azole groups in various heterocycles have compelling hydrophobicity and pharmacokinetic properties that impart transmembrane diffusion ability to the drug to reach the target [1]. Pyrazoles are indispensable members of the azole class having two adjacent nitrogen and three carbon atoms with a five-membered ring. The pyrazole scaffold can be better understood in scheme1 as shown below. The N-1 atom in the structure is "pyrrole-like" because of its unshared electrons are conjugated with the aromatic system while, the N-2 atom is "pyridine-like" as the paired electrons are not compromised with resonance, similar to pyridine systems. Due to such differences in the N-atoms, pyrazoles are reactive against both acids and bases [4].

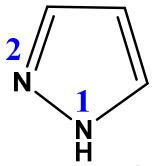

Scheme 1: Pyrazole skeleton

Pyrazole, though bearing high biological activity, is rarely found in nature because of the difficulty faced by living organisms to form N-N bond [5]. Synthesis of the first pyrazole derived compound was reported in 1883 which was later followed by its usage in therapeutics [2]. A few primitive examples of naturally occurring pyrazoles were: one as an isomer of histidine, isolated from the juice of watermelon from Citrulus vulgaris [5] and the other as 3-Nonyl-1H-pyrazole, extracted from Houttuynia cordata, which is a common plant in tropical Asia [4].

Pyrazoles and its derivatives are an important class of heterocyclic compounds which have immense scope in various biological activities and catalysis due to their ability to coordinate metal ions [6] and form complexes with metals like Pt, Pd, Cu, Zn, Au, Co, Ni, Fe, Ga and Au [7]. Scientists across the globe have left no stone unturned in devising the different biological applications of these compounds including anti-inflammatory, antibacterial, analgesic, anti-cancer, anti-tumor, anti-glaucoma, cardio-vascular, anti-chagasic, anti-pyretic, anti-spasmodic, anti-neoplastic, anti-diabetic, anti-oxidant, anti-viral, anti-leishmanial, anti-parasitic and anti-allergic [2-19]. Certain classes of condensed pyrazoles such as pyrrolo pyrazoles, pyrazolo indoles, pyrazolo triazoles, pyrazolo isoindoles, pyrazolo pyrazolones have exhibited profound biological activities such as kinase inhibitors, topoisomerase I & II inhibitors, antitumorigenic, herbicides, pesticides and anti-bacterial agents [1,2,5,12]. Some

pyrazole-based drugs have been successfully tested against cyclin kinase and are into clinical trials for the treatment of human cancers [20]. The target for pyrazole as anticancer drug ranges from human telomerase reverse transcriptase [16], tyrosine kinase, cyclin dependent kinase, Aurora A. kinase, Activen receptor like kinase 5, Mitogen activated protein kinase to fibroblast growth factor, Apoptosis inducing factor, and tumor growth factor [21]. Some of the commercially popular pyrazole based drugs are Celecoxib (gastrointestinally safe NSAID, analgesic and COX-2 inhibitor), Tepoxalin (a NSAID to treat osteoarthritis), Deracoxib (to treat osteoarthritis in dogs) [3], Antipyrine, Phenylbutazone, Tepoxalin, Sildenafil (to treat erectile dysfunction), Dipyrone (analgesic and antipyretic) and Rimonabant (for obesity treatment).

Among all the biological activities, anti-inflammatory and anti-microbial activities are the most investigated behaviors of the pyrazole ring structure [22]. Quinolone-based drugs like ciprofloxacin, which have always been broad spectrum antibiotics, are now prone to resistance against the disease-causing microbes for whom pyrazoles are a good alternative which act upon DNA gyrase. Tanitame et.al had also successfully synthesized pyrazole-based drugs targeting DNA gyrase [23-26]. In continuation with our earlier work on triazole–substituted drugs [27-28], we have now focused on new pyrazole-based systems. Designing of new organic drugs has revealed the extensive applications of pyrazole-based compounds; therefore, we have performed initial computational analysis post in silico designing of some pyrazole-based molecules. Use of computational method allows us to validate and evaluate all aspects of drug discovery at this time. Researchers with proficiency in computational drug designing have a benefit of proposing new candidate quickly and at a cheaper value than others. When the structure of the target is predictable, then molecular docking is the best tool for the evaluation of possible proffered candidates [29]. The theoretical observed results should always be compared with a commercially available drug, like common antibiotic drug ciprofloxacin, to obtain a broad spectrum of comparative behavior.

Herein, we have designed 47 new pyrazole derivatives and performed their docking studies along with 15 reported analogs, keeping in mind the basic desirable features of a good pharmacophore: aromatic ring current, hydrophobic-hydrophilic substituents, H-bond acceptors and donors and optimum molecular weight. All the electronic interactions and drug likeliness behaviors have also been compared with commercially available ciprofloxacin drug which is effective against bacterial infections including S. enterica, S. aureus, and E. coli [24]. The predicted activities have been validated by experimental antimicrobial studies after synthesizing four parent structures. The detailed structural predictions, docking studies, and validation of the theoretically predicted

behaviors have been described in the present work. DFT calculations of the synthesized compounds have also been carried out to elaborately understand the difference in molecular conformations, post docking.

2. Experimental Section

2.1 Molecular docking studies

Antibiotic resistant gram positive bacteria such as *S. aureus*, *S. pnemoniae, enterococci* are causative agents of nosocomial infections and hospital acquired infections worldwide [30]. The commercially available drugs against *S. aureus* are Cephalothin, Amikacin, Gentamicin, Cefpirome, Chloramphenicol, Tetracycline, etc. [22], which are on the verge of impotency due to the increasing drug resistance by the bacterium. Therefore, we have concentrated our docking studies done on crystal structure of DNA gyrase of *S. aureus*.

The docking studies of the molecules were carried out using *Glide5.0* module of Schrödinger 11.5 software [31]. The ligands were docked against protein structure 2XCT taken from PDB database with a resolution 3.35 Å. The synthesized compound was further derivatized by substituting groups on the benzene ring and the pyrazole. These derivatives were also docked at the same site in the protein and the results were compared with compounds synthesized by Allison *et. al* [32] as well as with the standard drug ciprofloxacin. Out of the computationally designed compounds derived from 4 basic skeletons (N-1, N-2, R-1 and R-16), we have successfully synthesized the four aforementioned compounds.

2.2 DFT studies

Quantum mechanical calculations were performed for four synthesized compounds using DFT method, with the help of Gaussian 09 software, at Becke's three-parameter hybrid functional and correlation functional of Lee, Yang And Pan (B3LYP), with 6-311+G (d,p) basis set in gas phase [33-35]. The default optimization and SCF procedures were followed in the program execution. All the geometrical parameters and optimized structures were determined for the four parent pyrazole compounds [36-38]. Then, the pose obtained for these compounds after docking, were used for "Single point calculations" using DFT. A comparative analysis of the geometrical data of parent compounds in their global minima state (obtained by geometry optimization) with the energies of their post docking poses (bioactive minima) was also done. All the results pertaining to DFT studies were visualized through Gauss view 5.0 software [39].

2.3 Materials preparation and characterizations

All the starting materials and solvents: 5-aminoisophthalic acid (Sigma Aldrich), 4-hydrazinobenzoic acid (Sigma Aldrich), Sodium nitrite (CDH), Sodium sulphite (TCI), Phosphorus oxychloride (Sigma Aldrich), Potassium permanganate (CDH), Potassium carbonate (CDH), Ethyl acetate (Avra), Potassium hydroxide (Avra), Conc. HCl (CDH), 2,4-Pentanedione (TCI), Dimethylformamide (Avra), ethanol (Avra) and isopropanol (Avra) were used as purchased without any further purification. The IR spectra were obtained with KBr pellets on a Shimadzu FT-IR spectrometer. The mass spectra were collected with XEVO G2-XS QTOF mass spectrometer. ^{1}H and ^{13}C NMR were recorded at room temperature (298 K) on Bruker Avance-III spectrometer operating at 400 MHz. All the compounds are also characterized by UV-visible spectra measured from UV-Visible Spectrophotometer, Perkin Elmer (Fig. S8 in Supporting information).

Scheme 2

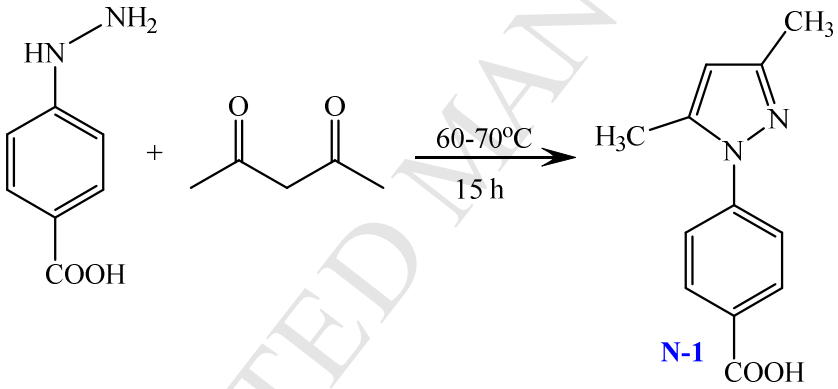

Synthesis of compound N-1: The compound N-1 was synthesized and characterized by earlier reported method [40].

Scheme 3

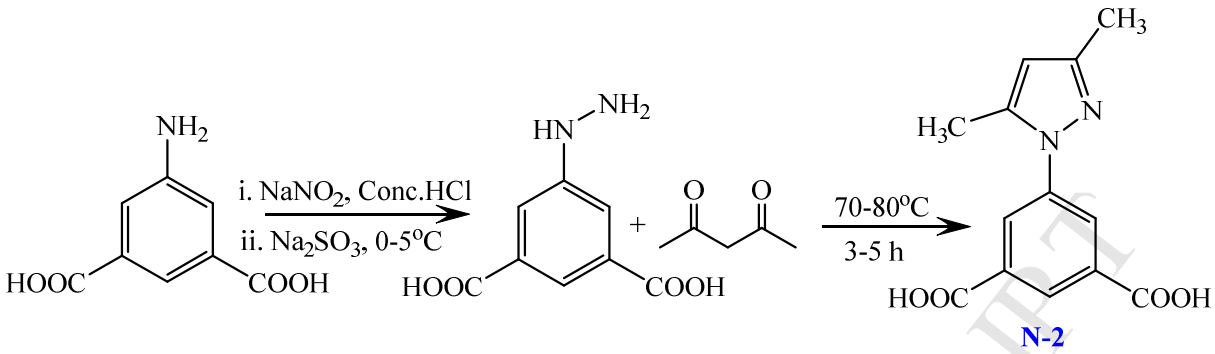

Synthesis of compound N-2: 5-aminoisophthalic acid (1g, 5.52 mmol) was suspended in ~6 mL water along with the addition of 1.5 mL conc. HCl. The resultant mixture was cooled at 0-5^{o}C with constant stirring for next 15 min. Then, 20 mL aqueous solution of sodium nitrite ($NaNO_2$, 0.36 g, 5.25 mmol) was added dropwise with controlled internal temperature 0-5^{o}C and stirred continuously for 1 h. In a separate beaker, sodium sulphite (Na_2SO_3, 1.75g, 13.9 mmol) was mixed with ~7 mL water and 2.8 mL conc. HCl. Then, the resulting sulphite mixture was added to the reaction mixture and the solution was stirred for next 1 h at 0-5^{o}C. After this, the reaction mixture was stirred at 60^{o}C for 3-5 h. The internal temperature was brought down to room temperature, followed by filtration and washing the product 4-5 times with distilled water. The washed product was air dried to obtain white colored 5-hydrazinyl-1, 3-benzene dicarboxylic acid with a yield of 95%. For the next step, 5-hydrazinyl-1, 3-benzene dicarboxylic acid (0.546 g, 3 mmol) and 2,4-pentanedione (0.34 mL, 3 mmol) were dissolved in isopropanol (20 mL) and refluxed for 3-5 h. The reaction mixture was filtered by using vacuum pump and it was air-dried to obtain pale yellow colored 5-(3, 5-dimethyl-1H-pyrazol-1-yl) 1,3-benzenedicarboxylic acid (N-2) compound with ~80% yield. The ligand structure was confirmed by using IR spectroscopy, mass spectrometry, ^{1}H NMR and ^{13}C NMR (DMSO-d^{6}) (see Supporting Information Fig. S1, S2, S3 and S4, respectively).

Scheme 4

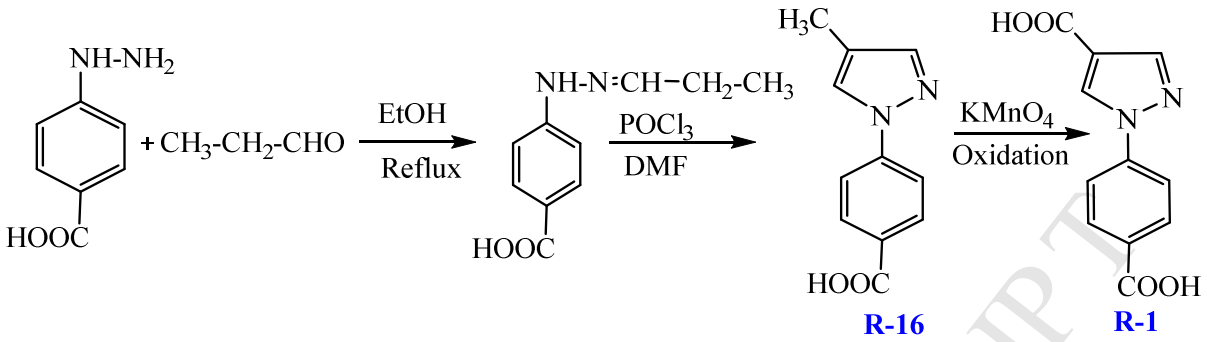

R-16 **R-1**

Synthesis of compound R-16 & R-1: 4-hydrazinybenzoic acid (1.065g, 14 mmol) and propionaldehyde (0.33 mL, 14 mmol) were refluxed in 35 mL ethanol for 4h at 70°C, and then the mixture was poured into 50 g ice-water mixture [41-43]. The yellow colored precipitate was collected with a yield of 0.94g (88%). In a separate beaker, the Vilsmeier-Haack reagent was prepared by adding of 0.87 mL (45 mmol) $POCl_3$ to 0.94 mL DMF at 0 °C in round-bottom flask in ice-cold condition (0-5°C) under constant stirring. Appropriate amount of 4-(2-propylidenehydrazinyl) benzoic acid, 0.6g (15 mmol) dissolved in 4 mL DMF were added to the Vilsmeier-Haack reagent and stirred for further an hour. Then, the reaction mixture was kept on an oil bath at 70 ºC for 4h. After the reaction, the mixture was poured into 20g of crushed ice under constant manual stirring. After neutralization with K_2CO_3 solution, ethyl acetate (30 mL) was added and the organic phase was separated from the aqueous phase by extraction with 60 mL AcOEt. The combined organic solutions were washed with water and brine, dried, and concentrated. Yellow colour solid 4-(4-methyl-1H-pyrazole-1-yl) benzoic acid (R-16) was collected with moderate yield. For the synthesis of 4-(4-methyl-1H-pyrazole-1-yl) benzoic acid (R-1), we took 4-(4-methyl-1H-pyrazole-1-yl) benzoic acid (R-16) 0.1g in pyridine (0.78 mL) and added a hot solution of potassium permanganate (0.97g) in H_2O (5.2 mL) at 115 °C along with constant stirring for 2h. After an additional 5h heating, the deposited manganese dioxide was filtered out and the product was washed with 0.3% aqueous KOH. The filtrate was collected and concentrated. After acidification with conc. HCl bringing down the pH to 1, the precipitated1-(4-carboxyphenyl)-1H-pyrazole-4-carboxylic acid (R-1) was filtered, washed with water, followed by acetone and dried. White colored solid was collected and the yield was found to be 0.015g. The decomposition temperature of the product was 250°C, and was soluble in DMSO. The ligand was confirmed by IR spectroscopy, mass spectrometry and ^{1}H NMR (DMSO-d^6) (see Supporting Information Fig. S5, S6 and S7). The UV-Vis spectra of all the four synthesized ligands (N-1, N-

2, R-1 & R-16) have also been collected and plotted against absorbance vs wavelength (see Supporting Information Fig. S8).

2.4 Anti-microbial activity

Two methods have been adopted for the determination of anti-microbial activity of the synthesized ligands. In anti-bacterial studies, the "Standard serial dilution" was adopted for determination of ligand potency against test bacterial strains [27,44]. The gram-positive strains were *S. aureus* (MTCC 3160), *B. subtilis* (MTCC 441), and gram negative strain were *E. coli* (MTCC 16521), *P. aeruginosa* (MTCC 424) and *S. enterica* (MTCC 3858). The potency of ligand against bacteria was compared to the MIC value of the standard drug Ciprofloxacin. In this method, the stock solution of 50µg/mL concentration was diluted to get a concentration of 25-1.56 µg/mL in different test tubes containing 1 mL of double strength nutrient broth. Then, these test tubes individually inoculated with 100 mL suspension of test microorganism in sterile saline. The test tubes were incubated undisturbed at 37 °C ± 1 for duration of 24 hours. Dimethyl sulfoxide (DMSO) was kept as solvent control.

Secondly, the anti-fungal activity of the synthesized molecule was evaluated against the most common fungal strains, *C. albicans* by the method of "Standard serial dilution" [28,45]. For *C. albicans*, freshly prepared fungal medium was taken into account to evaluate the anti-fungal activity using the agar well diffusion method. In this method, a plate of fungus was obtained from pure isolate and was allowed to grow at 37 °C for 24 h. 4 colonies from the plate were transferred into normal saline (0.85%) under sterile environment and the density of the suspension was adjusted to 10^6 cfu/mL (in accordance to 0.5 Mc Farland standard). This suspension was used as inoculum. For performing the assay 100 µL of the inoculum was swabbed on agar plates consisting of 20 mL agar, to achieve confluent fungal growth. The agar plates were dried and punched with sterile cork borer of 10 mm diameter to create wells for loading 100 µL of test sample with concentration of 8.0 mg/mL in 20% Dimethyl sulfoxide as solvent. The plates were incubated at 37 °C ±1 for 24 h, followed by evaluation of zone of growth inhibition with zone reader (Hi Antibiotic zone scale). Clomitrazole was taken as positive control for the fungus. The experiment was repeated for three times to minimize error. Dimethyl sulfoxide was taken as solvent control.

3. Results and discussion

3.1 Docking studies

A series of compounds were designed (Table S1, supporting information) and analyzed using latest version of *Glide 5.0* module of Schrodinger 11.5 software. We have designed four classes of compounds (N-1, N-2, R-1 & R-16) and have taken one class of reported compounds (A series) for the computational study. The designed molecules belonging to the S-series are also a derivative of the N-series. In N-1, a carboxylic acid group is present at para-position in phenyl ring with respect to the pyrazole ring and two methyl substituents are present at 3- and 5-positions in pyrazole ring. In N-2, there are two carboxylic acid groups at 3- and 5- positions on the benzene ring with respect to the pyrazole ring and two methyl substituents on the pyrazole ring similar to N-1. In case of R-1, there is one carboxylic group is present at para position similar to N-1 and a carboxylic group at the 4 position on the pyrazole ring. In R-16, the structure is quite similar to R-1 where the carboxylic acid group on the pyrazole is replaced by a lipophilic methyl group. All compounds were docked against DNA gyrase of *S. aureus* adopted from PDB file 2XCT. Here, 3.35Å structure complex satisfies our interest since it gives the complete tetrameric structure for DNA gyrase (A_2B_2) of *S. aureus* consisting of four active sites and 692 amino acids with a bound antibacterial drug molecule ciprofloxacin (Fig. S9 in Supporting Information). The DNA strands present in the crystal structure of DNA gyrase make it more versed in letting us to understand the intercalation of drug moiety in the active site of the protein and its interactions with components of DNA structure. Docking studies were performed on the four parent compounds (N-1, N-2, R-1, R-16) and certain derivatives of these compounds were designed to study the increased ligand-protein interactions along with any other existing electronic interactions (see Supporting information Fig. S10). The various substitutions of hydrophobic and hydrophilic groups in the aromatic rings can play a major role for the biological activity.

The compounds, N-1, N-2, R-1 and R-16 when evaluated on the basis of various interaction parameters through docking, show comparable results with the standard drug ciprofloxacin (Table 1). The major advantage of these molecules is the low molecular weight along with the retention of desirable properties like extensive hydrogen bonding (value is 1.2 in case of R-1 which is significantly high compared to ciprofloxacin). There is an H-bonding interaction of O-atom of one of the carboxylic acid groups of all the four ligands with the polar uncharged amino acid residue of Ser 1084 of the B-chain. The compounds containing carboxylic groups (as enlisted in Table S1) show similar hydrogen bonding interactions with DNA component. In case of R-1, there is additional hydrogen-bonding due to an extra carboxylic group substituted on the pyrazole ring, with Arg 458 residue of the B-chain. The pyrazole rings of the ligands show π-π stacking interactions with the nitrogenous bases of the DNA (DA H:13

fragment of DNA), denoted by the green arrow lines as shown in Fig. 1. Here, Mn^{+2} ion is present in protein pocket (a part of G-chain) which is mandatorily forming salt bridges with carbonyl and carboxyl oxygens of R-1 and carboxyl oxygens of N-1, N-2 and R-16. The metal coordination bond length is nearly 2.06 Å in case of N-1, R-1 and R-16 whereas it is 1.97 Å in case of N-2 (Fig. 2). This metal-coordination bond length is highly reduced in present compounds when compared to the standard drug (2.32 Å and 2.19 Å in case of ciprofloxacin), as shown in Fig. 3.

In order to improvise these interactions, the pyrazole structure was modified by changing the functional groups at various positions either in phenyl ring or in the pyrazole ring. The derivatization of the compounds was done computationally, followed by their docking at the same binding sites and evaluated their interaction scores in contrast to the standard drug ciprofloxacin. The results are compiled in Table S1 (see Supporting Information). If we try to get an insight of the various interaction scores obtained, we can observe that the compounds of the A-series have a comparatively poor M.W (Molecular weight) score than the rest which depend on the size of ligands. The interaction diagrams were analyzed for the compounds with highest H-bonding scores, like compounds R-1, R8, R22, S5, S6 and S7. Compounds exhibiting highest interactions at the docking site of DNA gyrase along with their respective scores are specified in Table 2. All the compounds have two interactions in common that are between the O-atom of the substituted carboxylic group and the Ser 1084 residue along with the salt bridging with Mn^{+2}. Compounds S7 and S6 show extensive H-bonding of their hydroxyl oxygen with Gly 458 and Asp 437 residue as well as oxygen of the substituted carboxyl group with Ser 1084. R8 shows a similar H-bonding interaction as R-1. In case of R22, S5 and S7 another contributor to the H-bonding interaction is the solvent exposure of the substituted F-atom. Compounds A8-A15 (excluding A13) though have good interaction scores in various parameters, the resultant score become low in the overall Glide score due to heavy penalty scores which is discussed later. The highest interactions were observed in case of S7 whereas the compound A14 showed the lowest favorable interactions.

When we carefully examine the interaction parameters of S7, A14 and standard drug ciprofloxacin, we observed pi-pi interactions between aromatic rings of the compounds and with the nitrogenous bases present in the DNA residues (DA H:13 DNA fragment) surrounding the molecules (as denoted by gray color, indicated as unspecified residues). The metal coordination bond and salt bridge between Mn^{+2} atom are present in the protein active site pocket which are mainly observed due to the presence of polar carboxylate groups of the compounds. The metal bond length is almost comparable in case of S7 and ciprofloxacin (i.e. 2.08 Å in S7 and 2.19 Å in the drug).

Compound S7 shows very strong H-bonding interactions with Ser 1084 and Gly 459 residue of the protein. Such kind of strong H-bond interactions are even not observed in the ciprofloxacin molecule, though it shows single such interaction with one of the DNA fragments DA H:13. The active site of the protein is flanked with five various amino acids: Arg 458 (B-chain) which is positively charged amino acid, Asp 437 and Glu 435, 477 (B-chain) which are negatively charged amino acids, Phe 1123 which is a hydrophobic amino acid, Gly 1082, 459(B-chain) which are nonpolar charged amino acids and Ser 1084 which is a polar uncharged amino acid. The compounds ciprofloxacin and S7 fit into the protein pocket to maximize their interactions with the favorable amino acid as observed in the Fig. 3. The occupancy of ligand S7 in protein pocket can be better understood using Fig. 5 and the interactions of ligand inside the protein pocket can be visualized from Fig. S12, S13 and Table S2 (see Supporting Information). The interaction diagram of compound A14 shows the certain familiar interactions like S7 compound, but it lags in overall score. As, the Cl^- ions are exposed to solvent which could have easily contributed in H-bond formation if present in the inner cavity. Its orientation does not suit the residues flanking it, giving it a high penalty score of 4 (refer Table S1 in Supporting information). If we observe the docking of all compounds at the active site of the protein, we can easily conclude that Ser 1084, Gly 1082 along with the DNA fragments are actively taking part for interactions with the drug molecules.

The compounds which exhibited the highest interactions with protein are given in Table 2. Most important parameter for measuring activity is the G-Score which signifies the total glide score that sums up all interaction values and deducting the penalties, lipophilicity (sum of the hydrophobic grid potential), H-bonding interactions, electrostatic interactions (including the electrostatic rewards), molecular weight (rewards for ligands with low molecular weights). The G-Score and related interaction values for all other docked molecules have been supplied in Table S1 (Supporting information). Interestingly, few compounds have been shown higher values of H-bonding interactions compared to standard drug ciprofloxacin. The G-score of the drug can be inferred from the high electrostatic interactions and the hydrophobicity as well. Here, compound S6 has electrostatic interaction score of -4.7 which is more than ciprofloxacin but it lags in the hydrophobicity thus deteriorating its overall G-Score. Low molecular weight is another advantage of our molecules over the standard drug which is obvious by the specified low M.W Score. Since, the protein exists as a tetramer with four chains, there are four binding sites of the drug in each of these chains. All of the parent compounds along with their derivatives were docked at these sites and a peculiar difference was observed in the G-score for each compound, which can draw us towards the conclusion that

even though the sites seem similar superficially but there might be difference in the interactions of the residues with these compounds. The above observations can be well explained by further computational and experimental studies discussed below.

3.2 Penalty Analysis

The *Glide 5.0* module offers a feature of highlighting penalty score for any ligand, at various grounds, during the process of docking. This analysis is important aspect of visualizing the faulty positioning of the functional groups in ligands with an attempt to rectify and improvise the interactions. A high penalty was charged for compounds A8 to A15 (excluding A13) on the basis of position of various protein residues and their ill interactions with the ligand functional groups. In case of A14, there is high penalty due to burial of charged group on the protein (referring to negatively charged amino acids like Glu 477 and Asp 437) by the ligand pertaining to minimum H-bond interactions made to the charged group. Also, there is a hydrophobic group of the ligand against donor groups of protein in a protein region which normally would give a favorable phobic packaging score. No such penalty was charged for compounds belonging to N and R series due to the appropriate positioning of the various lipophilic and hydrophilic moieties.

3.3 ADME analysis

The well-known ADME analysis i.e., Absorption (A), distribution (D), metabolism (M) and excretion (E) of any organic molecule is an important analysis which states about the disposition of any pharmaceutical compound inside an organism and therefore, influences the pharmacological activity of it [46]. In our work, this study was performed using Qikprop (ligand based ADME analysis) module of *Maestro 11.5*, which provides ranges for comparing particular molecule's properties with those of 95% of known drugs. The ADME analysis of all compounds in the data set was done. The parent compounds N-1, N-2, R-1 and R-1-6 show good drug like properties and no violations were observed in accordance to Lipinski's rule of five (as shown in Table 3). Other important properties of any pharmacologically active molecule, playing crucial role as drug candidate, are also taken into consideration like molecular weight, QPlogPw (which predicts water and gas partition coefficients), QPPCaco (which predicts permeability of a molecule for the gut-blood barrier through passive transport), percentage human oral absorption, globularity and the number of H-bonds that would be donated by the solute molecule to the water molecules in the aqueous solution (donor HB). The results of ADME analysis propound the theoretical drug-like behavior of these compounds which are very promising and can be considered beneficial for further laboratory

analysis of them. The top 20 candidates obtained after the interaction studies of molecules data set post docking were also subjected to ADME analysis (Table S3 in supporting information). They also exhibited similar behavior in comparison to the standard drug Ciprofloxacin, though some were showing improved donor HB ability with lesser molecular weights which were inferred previously in other sections as well. Moreover, the percentage of oral absorption for few molecules was another striking result which was enhanced in our molecules than the standard drug.

3.4 DFT studies

The optimized geometries, total energies and dipole moments of the parent molecules were obtained from the DFT calculations. The observed optimized geometries of the four parent compounds have been depicted in Table 4. The optimized structures are found without any imaginary frequency and hence, all are characterized in their minimum energy states on the potential energy surface. The single point calculations were performed by importing the docked pose structures. Since there were no alterations done in the imported pose, hence, the molecules depicted are in ionized state with the removal of polar hydrogens as observed in their docked pose. A similar set of calculations were also carried out after converting the imported poses into unionized states by addition of their polar hydrogens but there were very tiny differences in the energies as well as in the torsional angles. We have tabulated all the results obtained from the optimized structures and the post docked structures to observe the changes in their conformations and energies (Table 5). The values mentioned in column ‘a’ correspond to the optimized structure of the molecules whereas the values in column ‘b’ correspond to the values pertaining to the single point calculation studies performed with post docking molecules. The torsional angles mentioned in both the columns correspond to the similar angles, though the nomenclature may change for single point calculations of the post docked molecules due to the ionized structures after removal of polar hydrogen.

On comparison of the data obtained after geometry optimization and single point energy calculations for the same molecule, it is observed that, there are certain conformational changes observed in the molecule upon docking. These changes can be explained by the hypothesis that the structure obtained on geometry optimization is the ‘global minima’ whereas the one obtained after docking is the best suited pose resulted from the ligand interaction with the surrounding entities of protein pocket, which can be referred as the ‘bioactive minima’ [47]. On the comparison of the two molecules N1 and N2, their optimized structures are found to be completely overlapping with each other but the molecules are posing differently in the protein pocket (Fig. 7a). This can be attributed to the

mandatory interaction of the residue Gly 459 with –COOH group of substituted phenyl ring in case of N2 which can be better understood from Fig 7b. Such conformational variation results to a significant change in the torsional angles of the molecule, in order to remain in the vicinity of the interacting residues as mentioned in the Table 5. A correlation between total energies of the molecule and their respective interaction scores can be established as well. The lower energies were obtained in case of N2 (-24,852.08 e.V) and R1(-22,712.083 e.V), which are in the agreement with their G-scores obtained after docking. The lowest energy in the compound N2 is observed due to the presence of two –COOH groups playing a pivotal role in the better interaction behavior. Moreover, there is a constant trend of increase in dipole moment after docking in the each molecule.

3.5 Anti-microbial studies of synthesized compounds

To verify the veracity of our computational results, four parent compounds were successfully synthesized namely: **N-1** [5-(3,5-dimethyl-1H-pyrazol-1-yl)1,3-benzoic acid], **N-2** [5-(3,5-dimethyl-1H-pyrazol-1-yl)1,3-benzenedicarboxylic acid], **R-1**[1-(4-carboxyphenyl)-1H-pyrazole-4-carboxylic acid] and **R-16 [**4-(4-methyl-1H-pyrazole-1-yl)benzoic acid] as depicted in Table 6.

The anti-bacterial properties were concluded by the minimum inhibitory concentration (MIC) value of the synthesized molecule against different bacterial strains (as shown in Table 6). The anti-bacterial testing of the synthesized compounds revealed that the compounds were active against almost all strains of common bacteria (as Table 6). Compound N-2 is showing higher activity against *B. subtilis* and *P. aeruginosa* with a MIC value of 12.5 which is better than earlier reported compound N-1, though it was not tested for anti-bacterial activities before. Compound R-1 was found to be active against *S. enterica* and moderately active against all other bacterial strains. The MIC values for our standard drug ciprofloxacin against *E. coli, B. subtilis, S. aureus, P. aeruginosa and S. enterica* are 0.08, 0.06, 0.6, 0.15 and 0.06 µg/mL, respectively.

The anti-fungal activity was also measured for the best performing candidate N-2 (in the anti-bacterial testing) along with compound N-1. Although the compound N-2 showed promising anti-bacterial activity, the anti-fungal activity was better in case of N-1. The diffusion diameter was found to be 3 mm for compound N-2, whereas it was 10 mm for compound N-1 as shown in Fig. 8. Hence, compound N-2 can be a better anti-bacterial candidate but N1 is better anti-fungal drug.

4. Conclusions

Pyrazoles are an evolving class of azoles as antimicrobial agents due to the increasing resistance of pathogenic microbes to multiple drugs including ciprofloxacin. Therefore, an efficient strategy has been employed to design noble pyrazole based drug molecules, keeping in mind the basic pre-requisites of any good pharmacophore: aromaticity, optimum molecular weight, hydrophobic and hydrophilic substituents along with H-bond accepting and donating groups. On the basis of the computational analysis, a noble bunch of pyrazole based compounds have been propounded that could be good antimicrobial agents. Four parent skeletons have also been synthesized and studied anti-microbial testing against various gram-positive, gram-negative bacteria and a fungal species. Computational biological activity was well matched with preliminary experimental results. Structural optimizations of synthesized compounds have also been carried out to validate the conformational arrangement of the docked structures. The synthesis of other derivatives from these four compounds is under process. The current research on pyrazole based molecules can be a useful aid in the development of newer pyrazole based drug candidates for various laboratories and pharmaceutical industries in future.

Acknowledgements

Authors acknowledge the financial support from the Department of Science and Technology through INSPIRE Award (No. IFA14-CH-144) & Science and Engineering Research Board, India in the form of Start-Up Research Grant (No.SB/FT/CS-098/2014). AKP and NK are also thankful to UGC-DAE-CSR for support in various aspects.

Conflicts of interest

There are no conflicts to declare.

References

[1] M.J. Ahsan, J.G. Samy, H. Khalilullah, M.S. Nomani, P. Saraswat, R. Gaur, A. Singh, Molecular properties prediction and synthesis of novel 1,3,4-oxadiazole analogues as potent anti-microbial and antitubercular agents, Bioorg. Med. Chem. Lett. 21 (2011) 7246–7250. doi:10.1016/j.bmcl.2011.10.057.

[2] A.M. Al-Azzawi, A. Sa'adi Hassan, Synthesis and antimicrobial actvity of new succinimides bearing different heterocycles, IJRPC 2014, 4(4), (2014) 755–762. www.ijrpc.com.

[3] S.G. Kücükgüzel, S. Senkardes, Recent advances in bioactive pyrazoles, Eur. J. Med. Chem. 97 (2015) 786–815. doi:10.1016/j.ejmech.2014.11.059.

[4] J.V. Faria, P.F. Vegi, A.G.C. Miguita, M.S. dos Santos, N. Boechat, A.M.R. Bernardino, Recently reported biological activities of pyrazole compounds, Bioorg. Med. Chem. 25 (2017) 5891–5903.

doi:10.1016/j.bmc.2017.09.035.

[5] V. Kumar, K. Kaur, G.K. Gupta, A.K. Sharma, Pyrazole containing natural products: Synthetic preview and biological significance, Eur. J. Med. Chem. 69 (2013) 735–753. doi:10.1016/j.ejmech.2013.08.053.

[6] A. Kufelnicki, M. Woźniczka, L. Chęcińska, M. Miernicka, E. Budzisz, Synthesis and structure of novel copper(II) complexes with pyrazole derived ligands and metal–ligand interaction in solution, Polyhedron. 26 (2007) 2589–2596. doi:10.1016/j.poly.2006.12.043.

[7] F.K. Keter, J. Darkwa, Perspective: the potential of pyrazole-based compounds in medicine, BioMetals. 25 (2012) 9–21. doi:10.1007/s10534-011-9496-4.

[8] B.M. Chougala, S. Samundeeswari, M. Holiyachi, L.A. Shastri, S. Dodamani, S. Jalalpure, S.R. Dixit, S.D. Joshi, V.A. Sunagar, Synthesis, characterization and molecular docking studies of substituted 4-coumarinylpyrano[2,3-c]pyrazole derivatives as potent anti-bacterial and anti-inflammatory agents, Eur. J. Med. Chem. 125 (2017) 101–116. doi:10.1016/j.ejmech.2016.09.021.

[9] N.C. Desai, D.D. Pandya, V. V. Joshi, K.M. Rajpara, H. V. Vaghani, H.M. Satodiya, Synthesis, characterization and anti-microbial screening of hybrid molecules containing benzimidazole-pyrazole and pyridine nucleus, Med. Chem. Res. 21 (2012) 4463–4472. doi:10.1007/s00044-012-9990-4.

[10] S. Domiati, A. El-Mallah, A. Ghoneim, A. Bekhit, H.A. El Razik, Evaluation of anti-inflammatory, analgesic activities, and side effects of some pyrazole derivatives, Inflammopharmacology. 24 (2016) 163–172. doi:10.1007/s10787-016-0270-7.

[11] B.P. Bandgar, S.S. Gawande, R.G. Bodade, N.M. Gawande, C.N. Khobragade, Synthesis and biological evaluation of a novel series of pyrazole chalcones as anti-inflammatory, antioxidant and anti-microbial agents, Bioorg. Med. Chem. 17 (2009) 8168–8173. doi:10.1016/j.bmc.2009.10.035.

[12] D. Raffa, B. Maggio, M.V. Raimondi, S. Cascioferro, F. Plescia, G. Cancemi, G. Daidone, Recent advanced in bioactive systems containing pyrazole fused with a five membered heterocycle, Eur. J. Med. Chem. 97 (2015) 732–746. doi:10.1016/j.ejmech.2014.12.023.

[13] M.F. Khan, M.M. Alam, G. Verma, W. Akhtar, M. Akhter, M. Shaquiquzzaman, The therapeutic voyage of pyrazole and its analogs: A review, Eur. J. Med. Chem. 120 (2016) 170–201. doi:10.1016/j.ejmech.2016.04.077.

[14] M.E.A. Zaki, H.A. Soliman, O.A. Hiekal, A.E. Rashad, Pyrazolopyranopyrimidines as a Class of Anti-

Inflammatory Agents, Zeitschrift Für Naturforschung C, 61c) 1–5 (2006). doi:10.1515/znc-2006-1-201.

[15] M. Li, B.-X. Zhao, Progress of the synthesis of condensed pyrazole derivatives (from 2010 to mid-2013), Eur. J. Med. Chem. 85 (2014) 311–340. doi:10.1016/j.ejmech.2014.07.102.

[16] J.B. Shi, W.J. Tang, X.B. Qi, R. Li, X.H. Liu, Novel pyrazole-5-carboxamide and pyrazole–pyrimidine derivatives: Synthesis and anticancer activity, Eur. J. Med. Chem. 90 (2015) 889–896. doi:10.1016/j.ejmech.2014.12.013.

[17] X.-H. Lv, Z.-L. Ren, B.-G. Zhou, Q.-S. Li, M.-J. Chu, D.-H. Liu, K. Mo, L.-S. Zhang, X.-K. Yao, H.-Q. Cao, Discovery of N -(benzyloxy)-1,3-diphenyl-1 H -pyrazole-4-carboxamide derivatives as potential antiproliferative agents by inhibiting MEK, Bioorg. Med. Chem. 24 (2016) 4652–4659. doi:10.1016/j.bmc.2016.08.002.

[18] N. Ghareb, H.A. Elshihawy, M.M. Abdel-Daim, M.A. Helal, Novel pyrazoles and pyrazolo[1,2-a]pyridazines as selective COX-2 inhibitors; Ultrasound-assisted synthesis, biological evaluation, and DFT calculations, Bioorg. Med. Chem. Lett. 27 (2017) 2377–2383. doi: 10.1016/j.bmcl.2017.04.020

[19] N. Ghareb, M.M. Abdel-Daim, N.M. El-Sayed, M.S. Elgawish, Synthesis, molecular modelling, and preliminary anticonvulsant activity evaluation of novel naphthalen-2-yl acetate and 1, 6-dithia-4, 9-diazaspiro [4.4]nonane-3, 8-dione derivatives, Bioorg. Med. Chem. Lett. 71(2017) 110-119. doi: 10.1016/j.bioorg.2017.01.018.

[20] P.G. Wyatt, A.J. Woodhead, V. Berdini, J.A. Boulstridge, M.G. Carr, D.M. Cross, D.J. Davis, L.A. Devine, T.R. Early, R.E. Feltell, E.J. Lewis, R.L. McMenamin, E.F. Navarro, M.A. O'Brien, M. O'Reilly, M. Reule, G. Saxty, L.C.A. Seavers, D.-M. Smith, M.S. Squires, G. Trewartha, M.T. Walker, A.J.A. Woolford, Identification of N -(4-Piperidinyl)-4-(2,6-dichlorobenzoylamino)-1 H -pyrazole-3-carboxamide (AT7519), a Novel Cyclin Dependent Kinase Inhibitor Using Fragment-Based X-Ray Crystallography and Structure Based Drug Design, J. Med. Chem. 51 (2008) 4986–4999. doi:10.1021/jm800382h.

[21] H. Kumar, D. Saini, S. Jain, N. Jain, Pyrazole scaffold: A remarkable tool in the development of anticancer agents, Eur. J. Med. Chem. 70 (2013) 248–258. doi:10.1016/j.ejmech.2013.10.004.

[22] F. Abrigach, Y. Rokni, A. Takfaoui, M. Khoutoul, H. Doucet, A. Asehraou, R. Touzani, In vitro screening, homology modeling and molecular docking studies of some pyrazole and imidazole derivatives, Biomed. Pharmacother. 103 (2018) 653–661. doi:10.1016/j.biopha.2018.04.061.

[23] J. Vashist, Vishvanath, R. Kapoor, A. Kapil, R. Yennamalli, N. Subbarao, M.R. Rajeswari, Interaction of nalidixic acid and ciprofloxacin wild type and mutated quinolone-resistance-determining region of DNA gyrase A, Indian J. Biochem. Biophys. 46 (2009) 147-153.ISSN: 0301-1208.

[24] A. Tanitame, Y. Oyamada, K. Ofuji, M. Fujimoto, K. Suzuki, T. Ueda, H. Terauchi, M. Kawasaki, K. Nagai, M. Wachi, J. Yamagishi, Synthesis and anti-bacterial activity of novel and potent DNA gyrase inhibitors with azole ring, Bioorg. Med. Chem. 12 (2004) 5515–5524. doi:10.1016/j.bmc.2004.08.010.

[25] S.L. Badshah, A. Ullah, New developments in non-quinolone-based antibiotics for the inhibiton of bacterial gyrase and topoisomerase IV, Eur. J. Med. Chem. 152 (2018) 393–400. doi:10.1016/j.ejmech.2018.04.059.

[26] J.J. Barker, Anti-bacterial drug discovery and structure-based design, Drug Discov. Today. 11 (2006) 391–404. doi:10.1016/j.drudis.2006.03.001.

[27] P. Yadav, K. Lal, L. Kumar, A. Kumar, A. Kumar, A.K. Paul, R. Kumar, Synthesis, crystal structure and antimicrobial potential of some fluorinated chalcone-1,2,3-triazole conjugates, Eur. J. Med. Chem. 155 (2018) 263–274. doi:10.1016/j.ejmech.2018.05.055.

[28] K, Lal, P. Yadav, A. Kumar, A. Kumar, A.K. Paul, Design, synthesis, characterization, antimicrobial evaluation and molecular modeling studies of some dehydroacetic acid-chalcone-1,2,3-triazole hybrids, Bioorg. Chem., 77 (2018), 236-244. doi:10.1016/j.bioorg.2018.01.016.

[29] W.L. Jorgensen, The Many Roles of Computation in Drug Discovery, Science 303(5665) (2004) 1813–1818. doi:10.1126/science.1096361.

[30] A. Barakat, A.M. Al-Majid, B.M. Al-Qahtany, M. Ali, M. Teleb, M.H. Al-Agamy, S. Naz, Z. Ul-Haq, Synthesis, anti-microbial activity, pharmacophore modeling and molecular docking studies of new pyrazole-dimedone hybrid architectures, Chem. Cent. J. 12 (2018) 29. doi:10.1186/s13065-018-0399-0.

[31] Schrödinger Release 2018-4: Glide, Phase, Ligprep, Schrödinger, LLC, New York, NY, 2018.

[32] D. Allison, E. Delancey, H. Ramey, C. Williams, Z.A. Alsharif, H. Al-Khattabi, A. Ontko, D. Gilmore, M.A. Alam, Synthesis and anti-microbial studies of novel derivatives of 4-(4-formyl-3-phenyl-1H-pyrazole-1yl) benzoic acid as potent anti-Acinetobacter baumannii agents, Bioorg. Med. Chem. Lett. 27(3) (2017) 387-392. doi:10.1016/j.bmcl.2016.12.068.

[33] M.J. Frisch, G.W. Trucks, H.B. Schlegel, G.E. Scuseria, M.A. Robb, J.R. Cheeseman, G. Scalmani, V. Barone, B. Mennucci, G.A. Petersson, H. Nakatsuji, M. Caricato, X. Li, H.P. Hratchian, A.F. Izmaylov, J.

Bloino, G. Zheng, J.L. Sonnenberg, M. Hada, M. Ehara, K. Toyota, R. Fukuda, J. Hasegawa, M. Ishida, T. Nakajima, Y. Honda, O. Kitao, H. Nakai, T. Vreven, J.A. Jr. Montgomery, J.E. Peralta, F. Ogliaro, M. Bearpark, J.J. Heyd, E. Brothers, K.N. Kudin, V.N. Staroverov, R. Kobayashi, J. Normand, K. Raghavachari, A. Rendell, J.C. Burant, S.S. Iyengar, J. Tomasi, M. Cossi, N. Rega, J.M. Millam, M. Klene, J.E. Knox, J.B. Cross, V. Bakken, C. Adamo, J. Jaramillo, R. Gomperts, R.E. Stratmann, O. Yazyev, A.J. Austin, R. Cammi, C. Pomelli, J.W. Ochterski, R.L. Martin, K. Morokuma, V. G. Zakrzewski, G.A. Voth, P. Salvador, J.J. Dannenberg, S. Dapprich, A.D. Daniels, O. Farkas, J.B. Foresman, J.V. Ortiz, J. Cioslowski, D.J. Fox, (2009) Gaussian 09, revision E.01; Gaussian, Inc.: Wallingford, CT.

[34] C. Lee, W. Yang, R.G. Parr, Development of the Colle-Salvetti correlation-energy formula into a functional of the electron density. Phys. Rev. B 37 (1988) 785-789. doi:10.1103/physrevb.37.785

[35] A. D. Becke. Density-functional thermochemistry. III. The role of exact exchange. J. Chem. Phys. 98 (1993) 5648–5652.doi:10.1063/1.464913

[36] M. Farag, A. M. Fahim, Synthesis. Biological evaluation and DFT calculation of novel pyrazole and pyrimidine derivatives, J. Mol. Struct. 1179 (2019) 304-314.

[37] S. Altürk, D. Avci, Ö. Tamer, Y. Atalay, 1H- pyrazole-3-carboxylic acid: Experimental and computational study, J. Mol. Struct. 1164 (2018) 28-36.

[38] S. Özkinali, M. Gür, N. Şener, S. Alkin, M. S. çavuş, Synthesis of new azo schiff bases of pyrazole derivatives and their spectroscopic and theoretical investigations, J. Mol. Struct. 1174 (2018) 74-83.

[39] Æ. Frisch, H. P. Hratchian, R. D. Dennington II, T. A. Keith, J. Millam, A. B. Nielsen, A. J. Holder and J. Hiscocks, GaussView 5 Reference, Gaussian, Inc., Wallingford, CT (2009).

[40] O. Moradei, I. Paquin, S. Leit, S. Frechette, A. Vaisburg, J.M. Besterman, P. Tessier, T.C. Mallais, Inhibitors of histone deacetylase, PCT Int. Appl. (2005) WO2005030704.

[41] J.P. Dusza, P.S. Chan, J.D. Albright, J.F. Bagli, A.A. Failli, M.A. Ashwell, A.J. Molinari, T.J. Caggiano, E.J. Trybulski, Preparation of benzodiazepines as vasopressin agonists for the treatment of diabetes insipidus, US Patent (2003) US 6511974 B1 20030128.

[42] J.K. Yoon, R.W. Saunders, M.B. Fawzi, Preparation and formulation of aryl 5H,11H-pyrrolo[2,1-c] [1,4] benzodiazepin-10-yl ketones and analogs as vasopressin agonists, PCT Int. Appl. (2001) WO 2001022969 A2 20010405.

[43] J.P. Dusza, J. Paul, P.S. Chan, J.D. Albright, J.F. Bagli, A.A. Failli, M.A. Ashwell, A.J. Molinari, J. Albert, T.J. Caggiano, E. J. Trybulski, Preparation of N-benzoylpyrrolobenzodiazepines and analogs as vasopressin V2 receptor agonists, PCT Int. Appl. (1999) WO 9906409 A1 19990211.

[44] C. P. Kaushik, K. Lal, A. Kumar, S. Kumar, Synthesis and biological evaluation of amino acid-linked 1,2,3-bistriazole conjugates as potential anti-microbial agents, Med. Chem. Res. 23 (2014) 2995–3004. doi: 10.1007/s00044-013-0882-z.

[45] K. R. Aneja, C. Sharma, R. Joshi, In vitro efficacy of amaltas (Cassia fistula L.) against the pathogens causing otitis externa, Jundishapur J. Microbiol. 4 (2011) 175-183.

[46] QikProp, version 3.5, Schrödinger, LLC, New York, NY, 2012.

[47] A. Ganjoo, C. Prabhakar, In silico structural anatomization of spleen tyrosine kinase inhibitors: Pharmacophore modeling, 3D QSAR analysis and molecular docking studies, J. Mol. Struct. 1189 (2019) 102-111. doi.org/10.1016/j.molstruc.2019.04.009

Table 1: Important docking parameters and corresponding scores for the four synthesized compounds N-1, N-2, R-1, R-16 and standard drug ciprofloxacin.

Compounds	**N-1**	**N-2**	**R-1**	**R-16**	**S.D.**
Structure	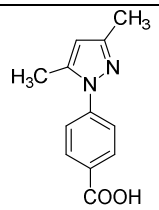	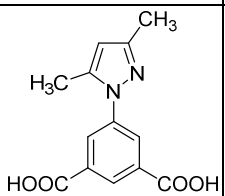	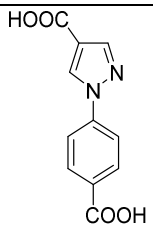	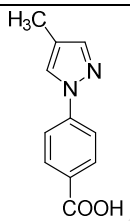	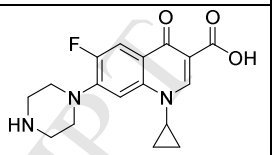
G-Score	-7.2	-7.5	-7.61	-7.02	-11.3
Electrostatic interactions	-3.0	-2.8	-2.8	-3.2	-4.58
H-bonding	-0.4	-0.3	-1.2	-0.5	-0.55
Lipophilic interactions	-3.4	-3.8	-3.1	-2.8	-4.27
Low M.W	-0.5	-0.5	-0.5	-0.5	-0.4

Table 2: Compounds with higher interactions at the docking site of DNA gyrase in *S. aureus*.

S. No.	Compound	Name Code	G-Score	Electrostatic interactions	H-Bonding	Lipophilic interactions	Low M.W
1.	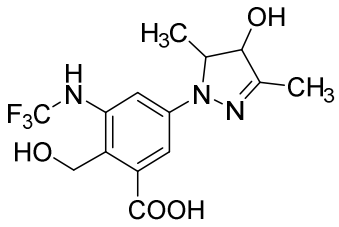	S7	-10	-4.4	-1.5	-3.8	-0.3
2.	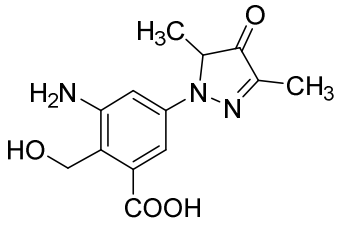	S6	-9.6	-4.7	-1.6	-2.5	-0.5
3.	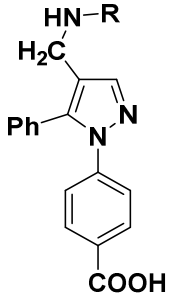 Where R= 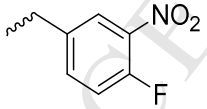	A13	-10.28	-3.76	-0.9	-4.06	-0.06
4.	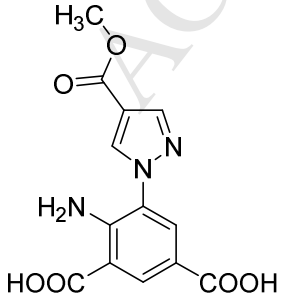	R11	-8.65	-2.94	-0.83	-4.39	-0.49

5.	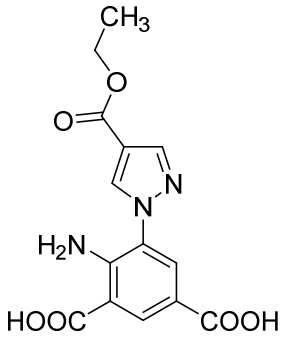	R12	-8.43	-2.95	-0.61	-4.42	-0.44
6.	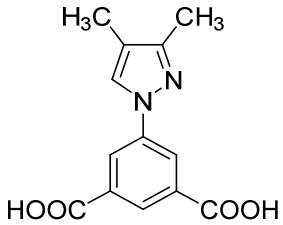	R18	-8.38	-2.96	-0.51	-4.41	-0.5
7.	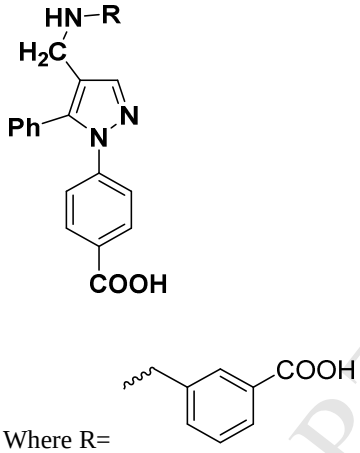 Where R=	A6	-8.33	-3.41	0.0	-4.79	-0.13
8.	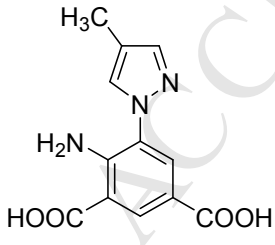	R21	-8.3	-3.12	-0.97	-3.72	-0.5

9.	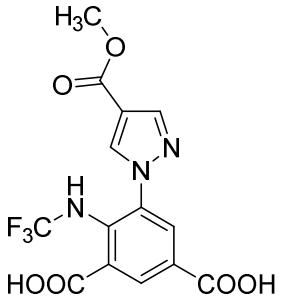	R24	-8.22	-3.16	-0.9	-3.91	-0.26
10.	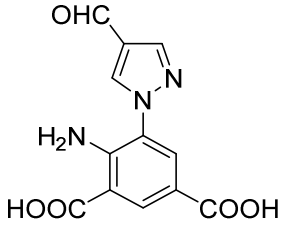	R15	-8.21	-2.8	-0.84	-4.07	-0.5
11.	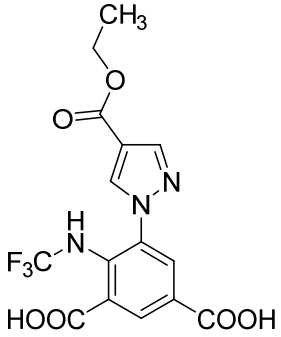	R25	-8.2	-2.86	-0.7	-4.42	-0.22
12.	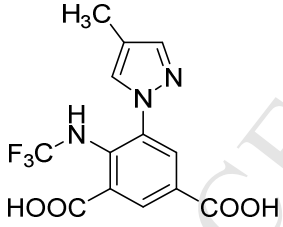	R23	-8.15	-2.91	-1.17	-3.66	-0.41

13.	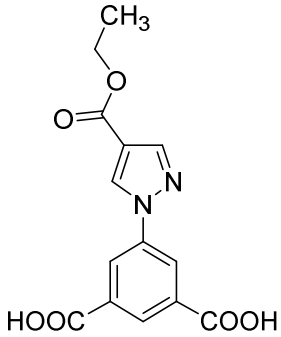	R6	-8.15	-2.93	-0.76	-3.97	-0.49
14.	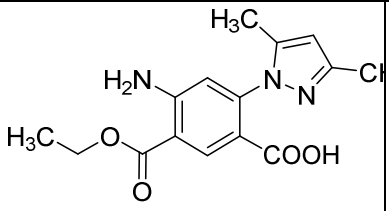	S11	-9.1	-4.0	0.0	-3.6	-0.5
15.	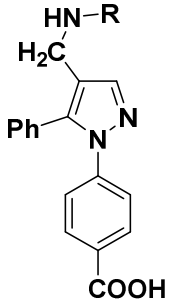 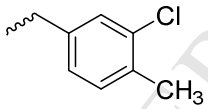 Where R=	A3	-8.12	-3.4	-0.63	-3.98	-0.11
16.	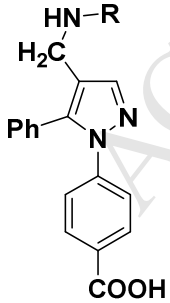 WhereR=	A2	-8.1	-3.63	-1.61	-3.73	-0.13

	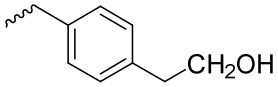						
17.	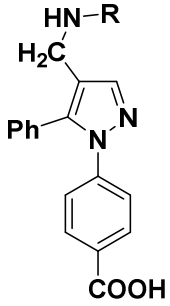 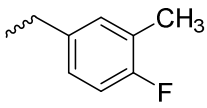 Where R=	A4	-8.07	-3.4	-0.64	-3.87	-0.17
18.	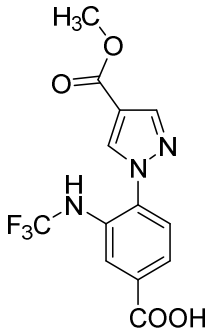	R26	-8.24	-3.28	-0.91	-3.64	-0.41
19.	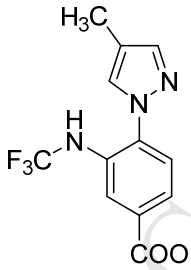	R22	-8.12	-3.4	-1.26	-3.15	-0.5
20.	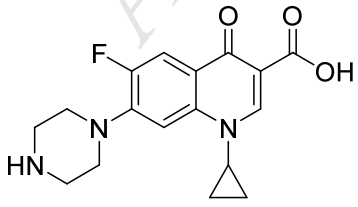	**S.D***	**-11.3**	**-4.58**	**-0.55**	**-4.27**	**-0.4**

Table 3: Various parameters obtained from ADME analysis of the four synthesized compounds N-1, N-2, R-1 and R-16.

S. No.	Molecules	M.W	QPlog Pw	QPPCaco	%Human oral Absorption	Rule of Five	Globin	Donor HB
1.	N-1	216.239	7.01	174.032	81.445	0	0.870	1
2.	N-2	260.239	10.616	4.691	50.103	0	0.857	2
3.	R-1	233.195	11.234	3.545	44.549	0	0.876	2
4.	R-16	202.212	7.284	156.838	79.728	0	0.878	1

Table 4: Comparative conformations after geometry optimization and after single point energy calculations of post docked structure.

Molecules	Optimized geometry	Single point calculation-based geometry
N1	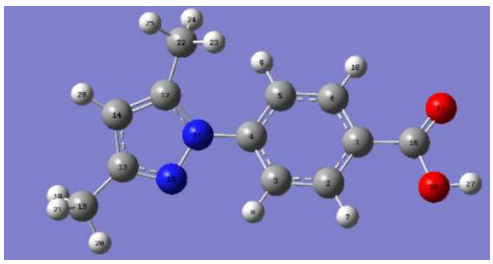	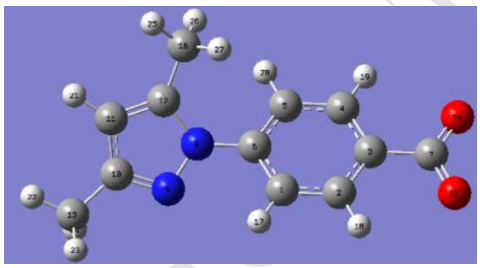
N2	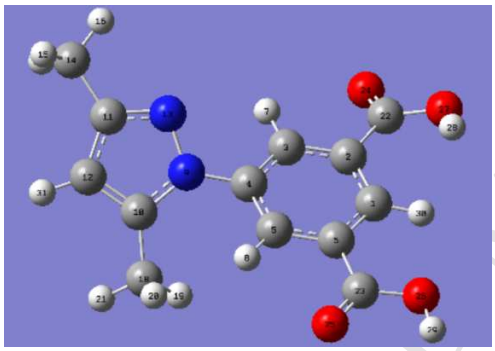	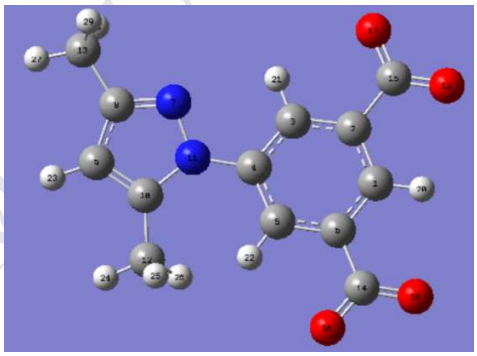
R1	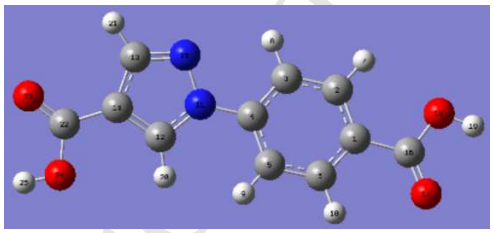	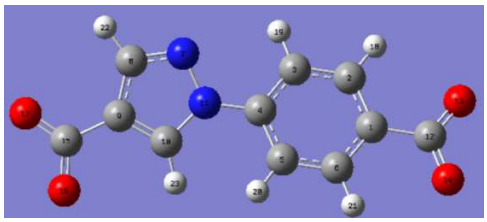
R16	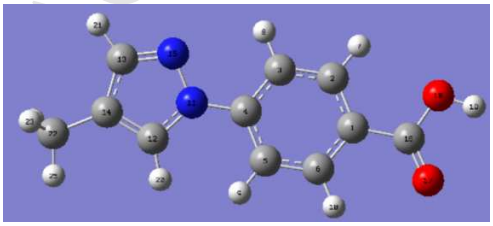	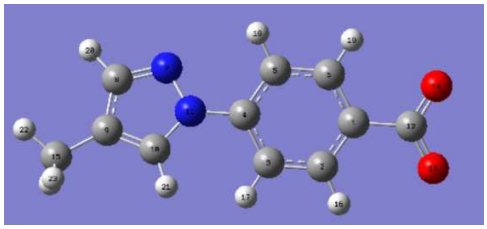

Table 5: Torsional angles and other parameters for four compounds after DFT study. The values in the columns (a) and (b) correspond to the results of the optimized structure and single point energy calculations, respectively.

B3LYP/6-311+G**										
N1			**N2**			**R1**			**R16**		
Parameters	Values		Parameters	Values		Parameters	Values		Parameters	Values	
DIHEDRAL ANGLES (°)	(a)	(b)	**DIHEDRAL ANGLES (°)**	(a)	(b)	**DIHEDRAL ANGLES (°)**	(a)	(b)	**DIHEDRAL ANGLES (°)**	(a)	(b)
C22 C12 N11 C4	0.14	-0.81	**C18 C10 N9 C4**	0.31	0.34	**O 24 C22 C14 C12**	0.55	2.14	**C22 C14 C12 N11**	179.78	177.68
						O24 C22 C14 C13	179.8	179.19	**C22 C14 C13 N15**	-179.62	-178.79
C18 C13 N15 N11	178.97	179.66	**C14 C11 N13 N9**	179.09	-178.7	**C12 N11 C4 C5**	-19.7	-21.64	**C12 N11 C4 C5**	-12.02	26.60
						C12 N11 C4 C3	160.5	156.45	**N15 N11 C4 C3**	-11.306	27.09
C12 N11 C4 C5	-38.07	-49.27	**C10 N9 C4 C5**	-38.69	-14.1	**N15 N11 C4 C3**	-18.7	-21.38	**O18 C16 C1 C6**	-179.70	-177.94
						N15 N11 C4 C5	161.07	160.54	**O18 C16 C1 C2**	0.14	2.27
C3 C4 N11 N15	-32.74	-47.44	**N13 N9 C4 C3**	-33.56	-11.33	**O18 C16 C1 C2**	0.10	-3.6			
						O18 C16 C1 C6	-179.67	176.18			

O26 C16 C1 C2	0.15	0.22	**O27 C22 C2 C3**	156.34	177.27					
			O27 C22 C2 C1	-26.11	-3.14					
O26 C16 C1 C6	-179.39	-179.71	**O26 C23 C6 C1**	0.82	-6.48					
			O26 C23 C6 C5	-178.44	175.91					
Energy (in e.V)	-19719.34	-19700.57	**Energy (in e.V)**	-24852.08	-24813.60	**Energy (in e.V)**	-22712.08	-22673.03	**Energy (in e.V)**	-18649.13	-18630.37
Dipole moment (in Debye)	2.54	5.00	**Dipole moment (in Debye)**	4.44	12.39	**Dipole moment (in Debye)**	1.51	1.76	**Dipole moment (in Debye)**	2.63	5.17

Table 6: *n vitro* anti-bacterial activities of four-synthesized compounds with their respective MIC values against various bacterial strains.

Compounds	**Structure**	***E. coli*** (µg/mL)	***B. subtilis***	***S. aureus***	***P. aeruginosa***	***S. enterica***
N-1 [5-(3,5-dimethyl-1H-pyrazol-1-yl)1,3-benzoic acid]	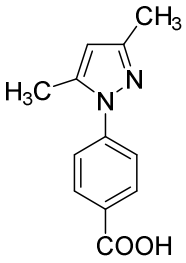	25	25	25	25	50
N-2 [5-(3,5-dimethyl-1H-pyrazol-1-yl)1,3-benzenedicarboxylic acid]	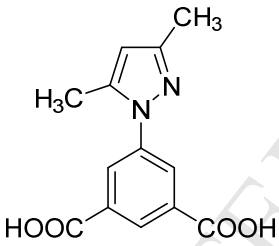	25	**12.5**	25	**12.5**	50
R-1[1-(4-carboxyphenyl)-1H-pyrazole-4-carboxylic acid]	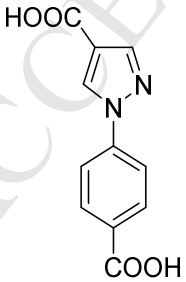	25	25	25	25	**12.5**

R-16[4-(4-methyl-1H-pyrazole-1-yl)benzoic acid]	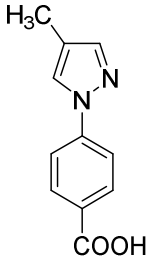	25	25	25		25

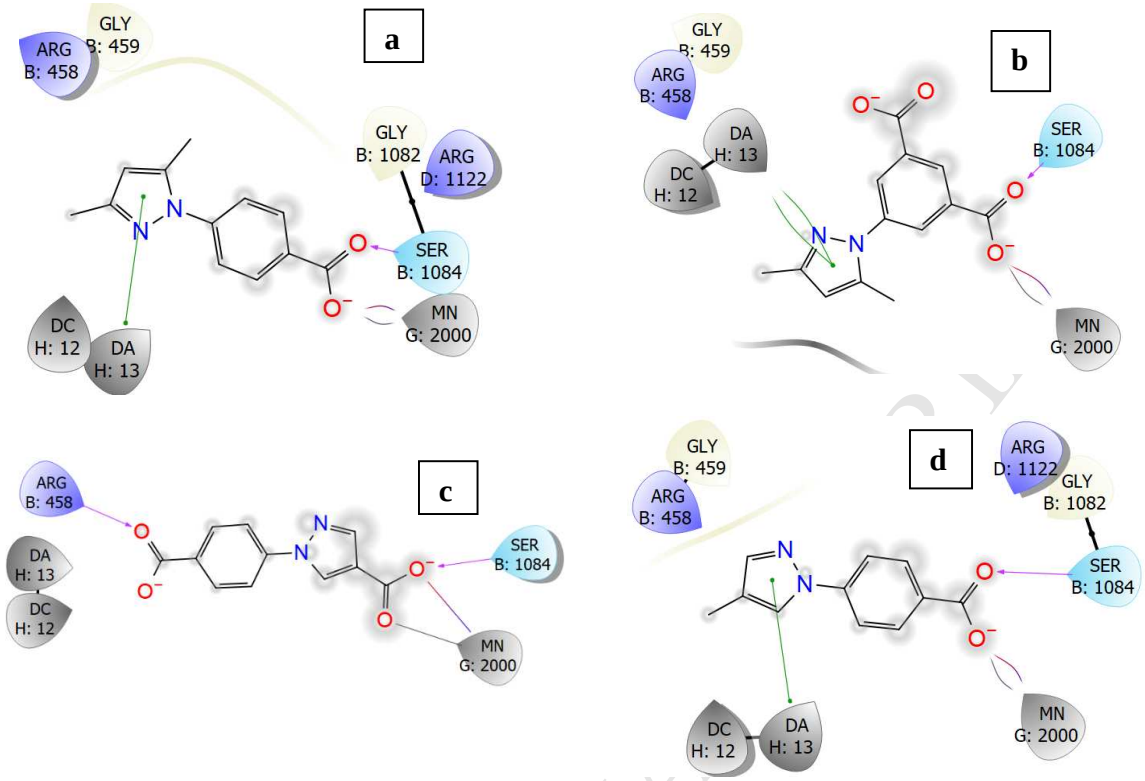

Fig. 1 The interactions of the protein complex with four parent molecules (a) N-1 (b) N-2 (c) R-1 and (d) R-16.

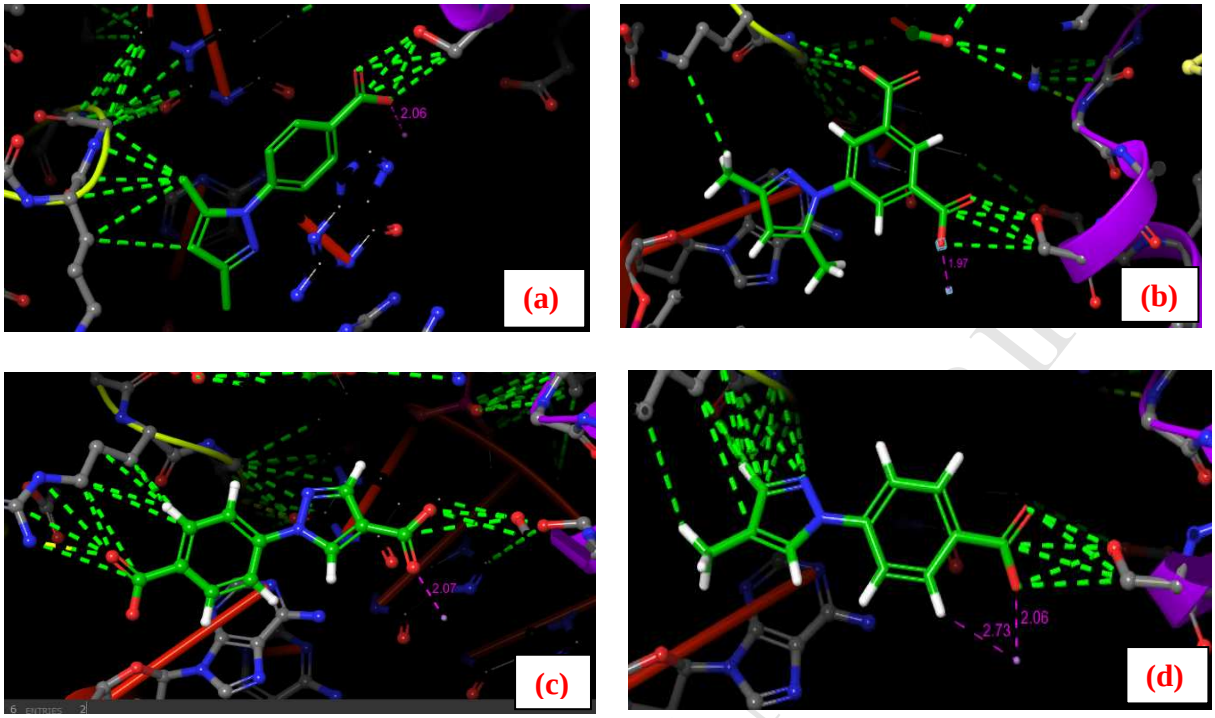

Fig. 2 The interaction diagram of parent compounds, (a) N-1 (b) N-2 (c) R-1 and (d) R-16 at the binding site of DNA gyrase in *S. aureus*. Note the green dotted lines for strong interactions. Blue, green, red and white wires represent N, C, O and H-atom, respectively.

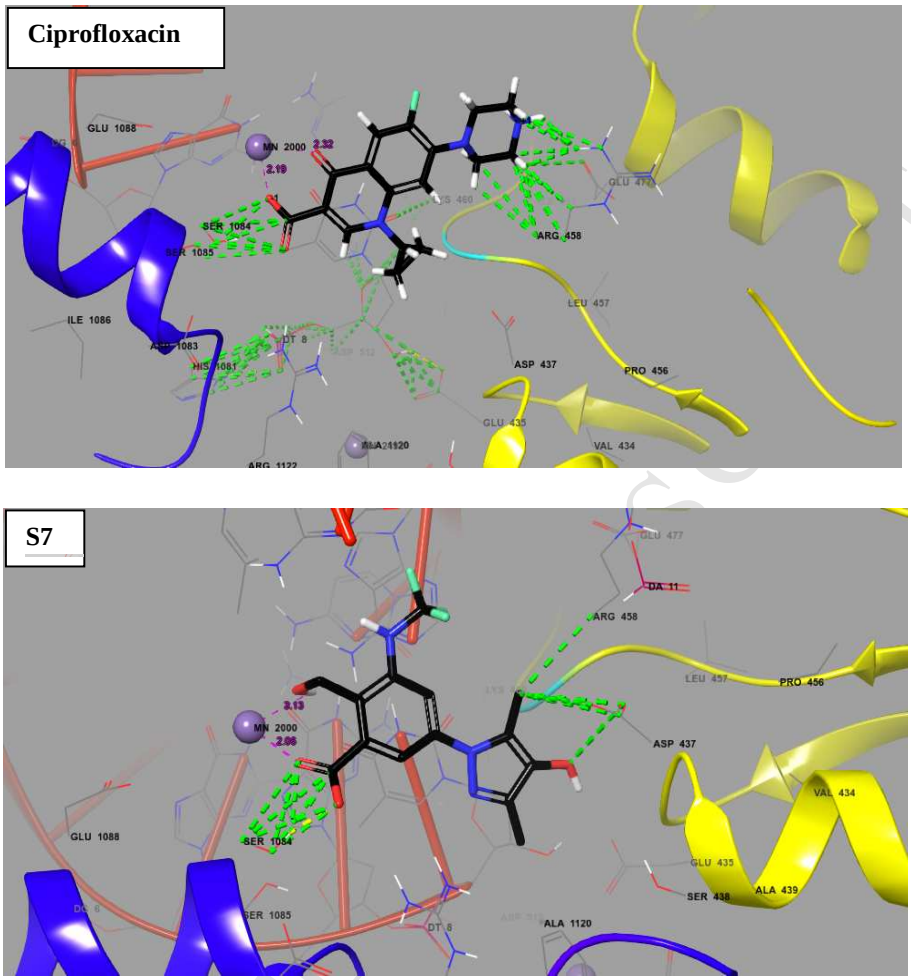

Fig. 3 Clear view for the interactions of ciprofloxacin and compound S7 within the protein pocket. The compounds are shown by thick wire presentation with oxygen atoms in red color, nitrogen atoms in blue color, Fluorine atom in green color, Hydrogen atoms in gray and the rest carbon framework in black color. The green lines demonstrate the strong interactions of the ligand with protein residues and DNA fragments with which it is flanked to.

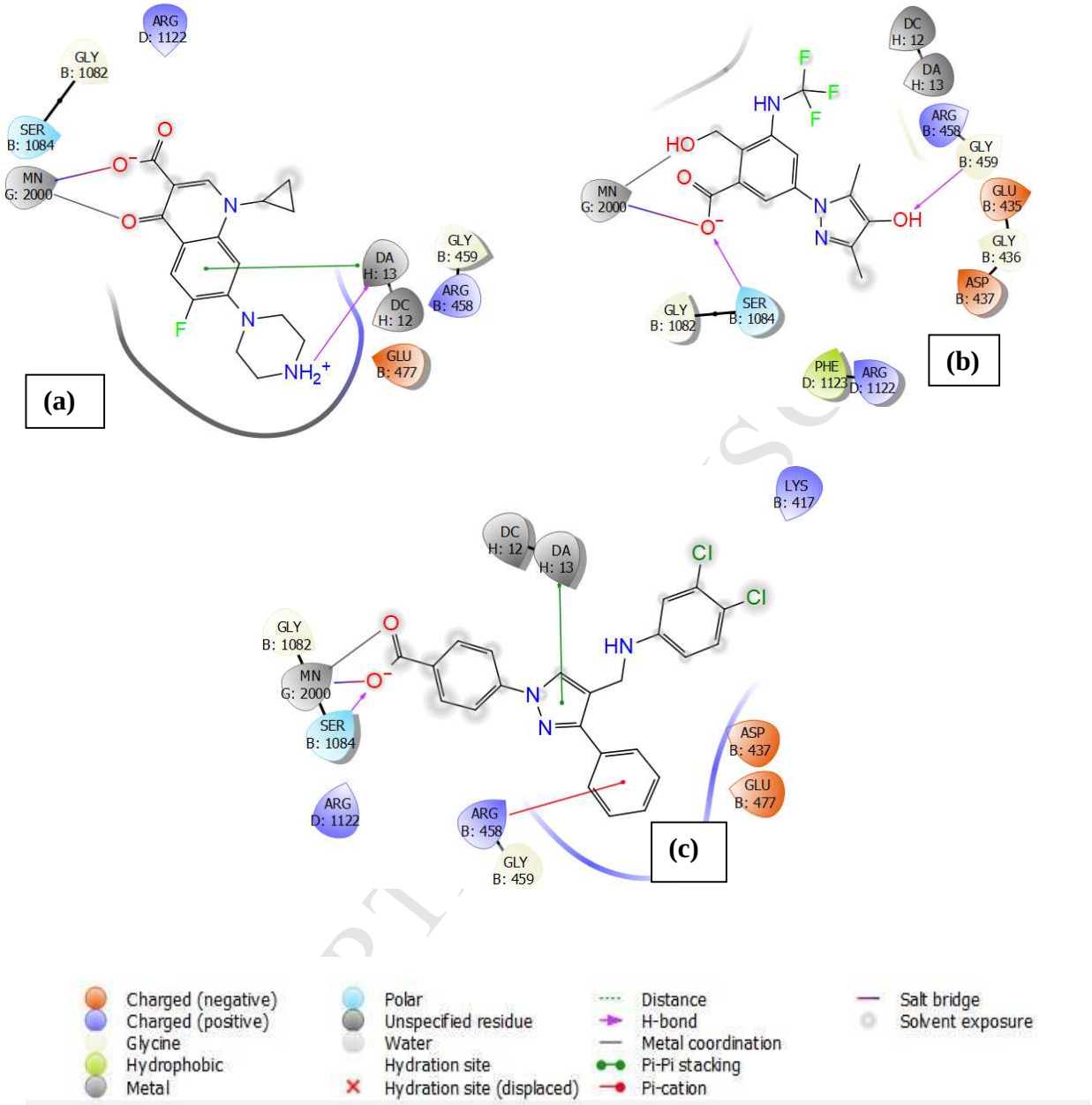

Fig. 4: Understanding the various interactions observed with the ciprofloxacin, compounds of highest and lowest G-scores (a) ciprofloxacin, (b) compound S7; (c) compound A14, respectively. Note the color annotations for the above interaction diagram.

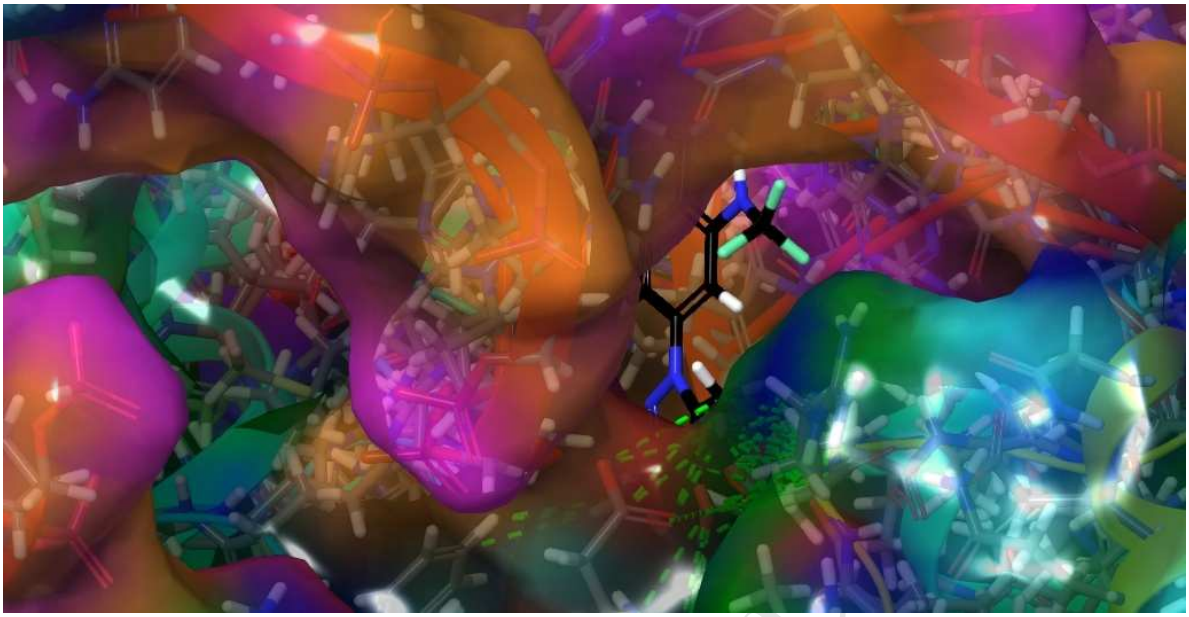

Fig. 5 Demonstrating the compound S7 fitting inside the protein pocket of DNA gyrase of *S. aureus*. The surface shows the protein part which is colored on the basis of residue property (consider Table S2 in supporting information for the color coding of the residues).

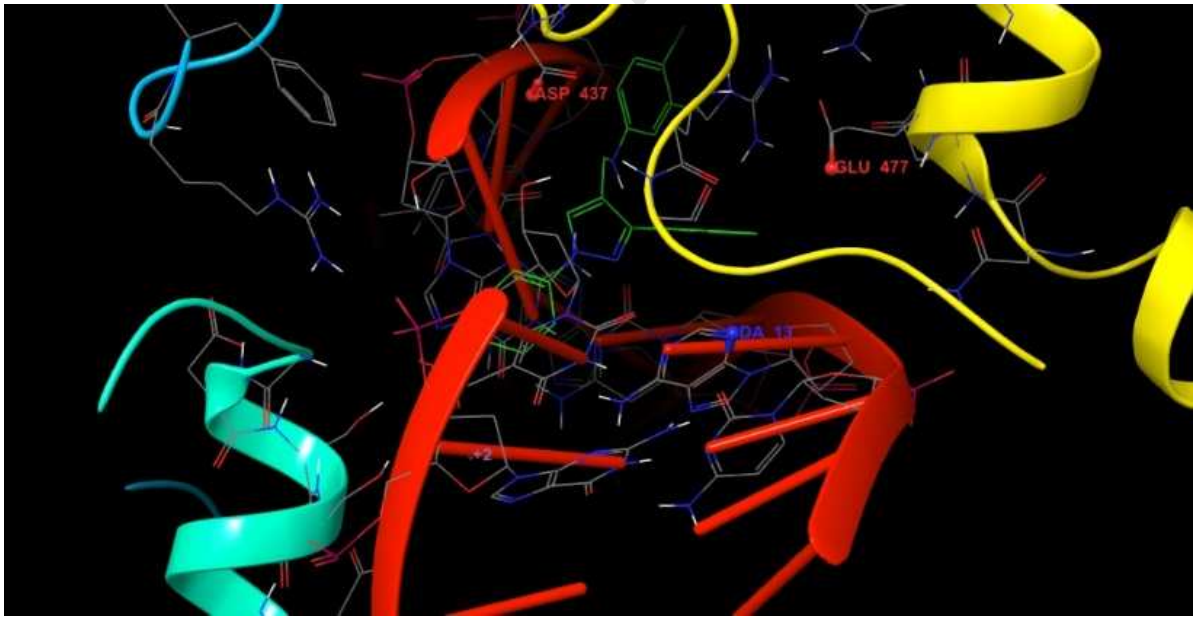

Fig. 6 Figure shows the interactions of ligand A14 with protein. Asp 437, Glu 477 residues of the protein are shown in red ball -stick representation and DA -13 DNA fragment with N-H group in blue ball-stick representation.

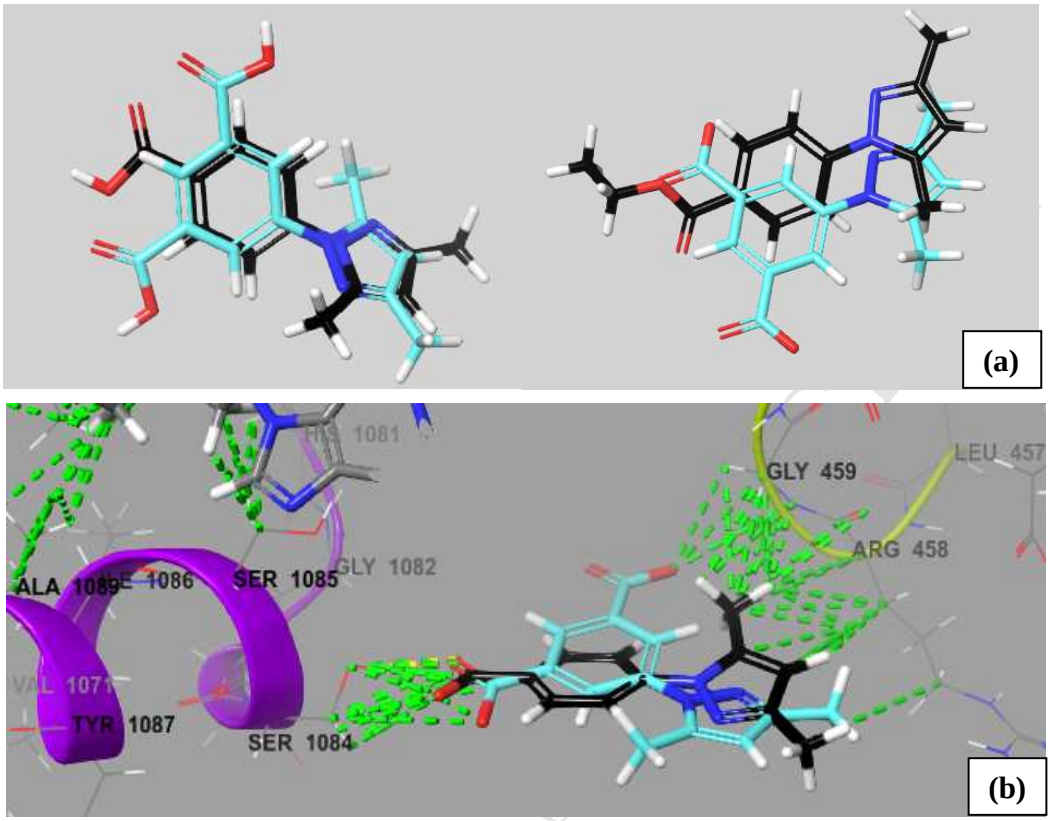

Fig. 7. (a) Comparison of molecular conformations of N1 and N2 structures before and after docking. Note the completely overlapped structures prior to docking. (b) Interactions for the stabilization in different conformation after docking.

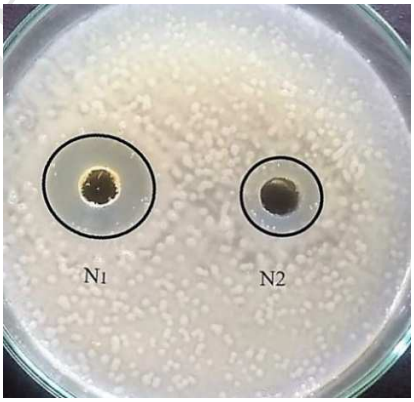

Fig. 8 Antifungal results of compound N-1 and N-2 against *C. albicans*.

Highlights:

- Series of biologically active pyrazole derivatives have been designed.
- Four pyrazole derivatives have been synthesized and characterized.
- Antimicrobial activity was tasted for the synthesized compounds.
- A good agreement between experimental activity and computational study was obtained.
- Docked poses and optimized conformations were compared by DFT study.